INFLUENCE OF SPACE CHARGE ON AXIAL PARTICLE MOTION IN HEAVY ION LINACS

P. Junior, H. Deitinghoff, H. Klein
Institut für Angewandte Physik der Universität Frankfurt/Main
D-6000 Frankfurt/Main, Germany

Summary

Considerations of beam dynamics for heavy ions within the frame of linear approximation at very low velocities are carried out. Decrease of acceptance due to space-charge for axial and radial motion is estimated. The behavior of idealized axial and radial beam envelopes with respect to space-charge and linac parameters is studied.

Necessity of Linear Theory

Theories of accelerator beam dynamics have always benefitted advantageously from the establishment of linear equations of motion. However, any linear approximation involves problems as soon as space-charge effects have to be considered. Yet, under certain assumptions, linear equations may still be used. For example; special geometric shapes of a particle beam permit the application of the well-known Kapchinskij-Vladimirkskij (K-V) model[1]. Within this frame Reiser derived his formula for the maximum charge in a FODO channel[2]. Adaptation to realistic charge distributions has been performed by Sacherer[3] and Lapostolle[4] using an RMS formalism. Basically, all these theories have to be restricted to transverse motion, requiring axial dimensions of the beam to be assumed large compared to transverse ones. This postulation seems violated in many linacs, especially at initial velocities, and certainly for the case of low charge state heavy ions in a fusion linac, where the axial envelopes are comparable to or smaller than the transverse ones. This paper discusses two models, deriving linear equations for the axial motion.

Linear theory in the presence of space-charge seems effective for many reasons. The many-body problem may be treated within the convenient frame of a comprehensive envelope representation, as only linear transformations conserve the ellipse character. This formalism collapses; however, as soon as at least one of the driving forces proves non-linear. The alternative is the use of long and expensive computational efforts. Validity and applicability of these models involve problems associated with the self-consistency of the theory.

Linac Models

For the first case, consider the K-V model[1], but replace one of the transverse motion components by the axial one. In the linac, assume a uniformly charged cylindric beam with an elliptic cross-section as Fig. 1 demonstrates. Axes are a_x, a_z, respectively. The beam does not move

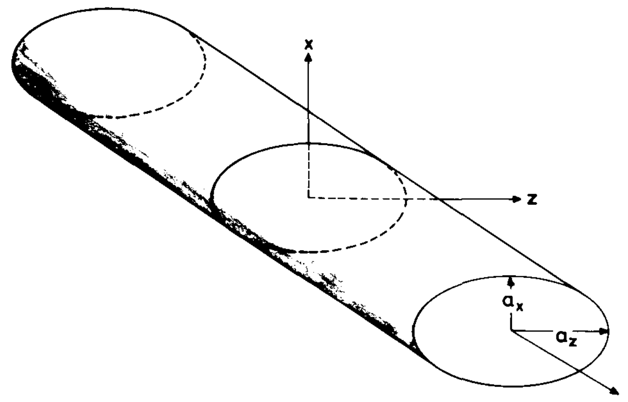

Fig. 1 Elliptic cylinder assigned to K-V model

along the y-direction but is accelerated transversely in the z-direction. Acceleration is provided by a plane wave, although it is understood that longitudinal plane electromagnetic waves do not exist. Dimensions should be regarded as infinite in the y-direction. With respect to Ref. 1, identical emittance areas in both phase space planes x-$\dot{x}$, z-$\dot{z}$ yield equations for axial and radial synchronous particles, respectively:

$$\frac{d^2z}{dt^2} + \frac{e}{m}\left(\frac{\omega}{v} E_o \sin\phi_s - \frac{3Q}{4\pi\varepsilon_o}\frac{F_z}{a_x^2 a_z}\right) z = 0 \qquad (1)$$

$$\frac{d^2x}{dt^2} - \left[\frac{e}{m}\left(\frac{\omega}{v} E_o \sin\phi_s + \frac{3Q}{4\pi\varepsilon_o}\frac{F_x}{a_x^2 a_z}\right) - D\right]x = 0 \qquad (2a)$$

There is a certain degree of freedom in the choice of a proper charge Q, which has been taken advantage of by cutting out of the beam rod a rotational ellipsoid with axes a_x, a_x, a_z, which fully contains Q, giving a relation for the uniform charge density ρ:

$$\rho = \frac{Q}{4/3\pi a_x^2 a_z}$$

Focusing is formally expressed by an elastic force Dx, where the elastic constant may be produced by an extended uniform axial magnetic field:

$$D = \frac{1}{4}\left(\frac{e}{m}\right)^2 B^2$$

An essential difference from Reference 1 must be pointed out. References 1 and 2 employ identical forces, disregarding the phase in the case of quadrupole lenses. Consequently, a restriction to identical emittance areas certainly proves to be unimportant in the K-V case, whereas, this means a severe restriction in the present case, as axial and radial emittance areas usually are not equal.

In Eqns. 1 and 2a form factors F_x and F_z were introduced, which are expressed as:

$$F_z = \frac{a_x}{a_x + a_z} \quad , \; F_x = 1 - F_z \tag{3a}$$

for the charge distribution of Fig. 1.

As a second model consider a uniformly charged ellipsoid with axes a_x, a_y, a_z as shown in Fig. 2. As with model 1, this form yields linear equations.

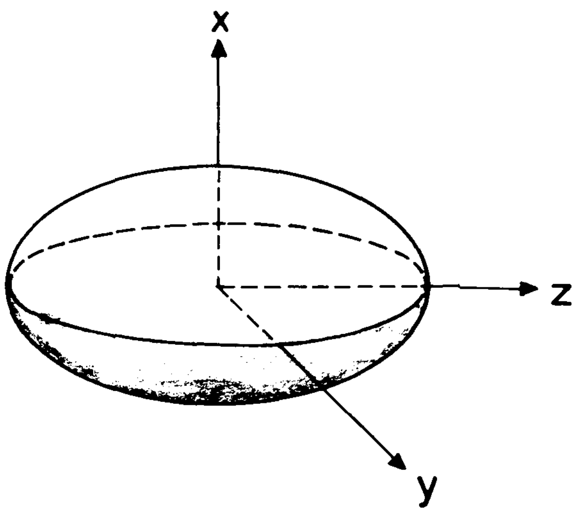

Fig. 2 Rotational ellipsoid as 3-dimensional beam model

Specifically, consider the case of rotational symmetry, $a_x = a_y$, admitting an identical axial equation (1), but a formally different radial equation[5,6,7]:

$$\frac{d^2x}{dt^2} - [\frac{e}{m} (\frac{1}{2} \frac{\omega}{v} E_o \sin\phi_s + \frac{3Q}{4\pi\varepsilon_o} \frac{F_x}{a_x^2 a_z}) - D] \; x = 0 \tag{2b}$$

and form factors

$$F_z = \frac{v^2}{\sqrt{1-v^2}^3}(\frac{1}{2} \ln\frac{1+\sqrt{1-v^2}}{1-\sqrt{1-v^2}} - \sqrt{1-v^2}) \; , v = \frac{a_x}{a_z} \leq 1$$

$$F_z = \frac{v^2}{\sqrt{v^2-1}^3} \; (\sqrt{v^2-1} - \arctan\sqrt{v^2-1}) \; , v = \frac{a_x}{a_z} \geq 1$$

$$F_x = \frac{1 - F_z}{2} \tag{3b}$$

In the general case of $a_x \neq a_y$ the equations are still linear, but the form factors have to be calculated numerically with elliptic integrals.

Self-Consistency

Beyond doubt the first model seems self-consistent, but an explanation should be inserted here. The space-charge field is assumed to be generated by the proper K-V particle distribution, covering the surface of a 4-dimensional ellipsoid, as will be shown later. Synchronous particles ($z = 0$, $\dot{z} = 0$) with respect to equations (2a), (2b) do not belong to these in general, but to some extent do not cause any disturbance of the external K-V field. This K-V distribution actually corresponds to the general equation:

$$\frac{d^2x}{dt^2} - [\frac{e}{m}(\frac{\omega}{v} E_o \sin\phi_s + \frac{\omega^2}{v^2} E_o z\cos\phi_s + \frac{3Q}{4\pi\varepsilon_o} \cdot \frac{F_x}{a_x^2 a_z}) - D]x = 0 \; ,$$

where a coupling term, $\omega^2 E_o z\cos\phi_s/v^2$, is added for the non-synchronous K-V particles. In this interpretation equations (1) and (2a) together with (3a) are still valid.

In Table 1, the course of analysis in Ref. 1 is extended to the cases of one and three dimensions. After comparing all columns of Table 1, it is seen that the uniformity of charge distribution in real space remains intact only when two dimensions are considered. Both of the other cases are not consistent with uniform charge distribution in real space; consequently, equations (1), (2b) in combination with (3b) describing Model 2, turn out non-realistic.

The following one-dimensional example shall illustrate this: for reasons of simplicity, take the emittance ellipse in the two-dimensional phase space to be on its principal axes. Additionally, units are chosen such that this ellipse becomes the unit circle. Electrical charge is distributed uniformly on the circle arc and according to Fig. 3a, the charge density projected on the x-axis appears non-uniform. This suggests a non-uniform charge distribution on the arc such that its projection becomes uniform, as Fig. 3b indicates. Now, taking this as a synchrotron ellipse, and transporting it through the corresponding optical system, all points in phase space, including those carrying charge, are rotated by an angle μ, where μ stands for the Flocquet exponent of the optical system[8,9]. Obviously the initially uniform charge density has turned out inhomogeneous after transport, as Fig. 3c illustrates. Thus, it appears as illogical in the case of 3-dimensions as it does for 1-dimension, to enforce uniformity of the charge distribution in real space, by laying on the surface of the corresponding 6-dimensional hyper-ellipsoid, an inhomogeneous charge distribution according to

$$(F_o - x^2/\delta_x^2 - y^2/\delta_y^2 - z^2/\delta_z^2)^{-\frac{1}{2}}$$

Table 1

Real space dimensions	1	2	3
Phase space dimensions	2	4	6
Ellipsoid equation in phase space	$(\delta_x \dot{x} - \dot{\delta}_x x)^2 + \frac{x^2}{\delta_x^2} = F$	$(\delta_x \dot{x} - \dot{\delta}_x x)^2 + \frac{x^2}{\delta_x^2}$ $+ (\delta_z \dot{z} - \dot{\delta}_z z)^2 + \frac{z^2}{\delta_z^2} = F$	$(\delta_x \dot{x} - \dot{\delta}_x x)^2 + \frac{x^2}{\delta_x^2}$ $+ (\delta_y \dot{y} - \dot{\delta}_y y)^2 + \frac{y^2}{\delta_y^2}$ $+ (\delta_z \dot{z} - \dot{\delta}_z z)^2 + \frac{z^2}{\delta_z^2} = F$
Charge density in phase space $n = n_o \delta(F - F_o)$	Uniform charge per arc unit length on plain 2-dimensional ellipse periphery F_o	Uniform charge per unit area on 4-dimensional ellipsoid surface F_o	Uniform charge per unit area on 6-dimensional ellipsoid surface F_o
Charge density in real space	$\rho(x) = \int n(x,\dot{x})\, d\dot{x}$	$\rho(x,z) = \int n(x,\dot{x},z,\dot{z})\, d\dot{x} d\dot{z}$	$\rho(x,y,z) = \int n(x,\dot{x},y,\dot{y},z,\dot{z})\, d\dot{x} d\dot{y} d\dot{z}$
Substitution polar coordinates	$\delta_x \dot{x} - \dot{\delta}_x x = \alpha$ $d\dot{x} = \frac{d\alpha}{\delta x}$	$\delta_x \dot{x} - \dot{\delta}_x x = \alpha\cos\phi$ $\delta_z \dot{z} - \dot{\delta}_z z = \alpha\sin\phi$ $d\dot{x} d\dot{z} = \frac{2\pi\alpha d\alpha}{\delta_x \delta_z}$	$\delta_x \dot{x} - \dot{\delta}_x x = \alpha\cos\phi\cos\theta$ $\delta_y \dot{y} - \dot{\delta}_y y = \alpha\sin\phi\cos\theta$ $\delta_z \dot{z} - \dot{\delta}_z z = \alpha\sin\theta$ $d\dot{x} d\dot{y} d\dot{z} = \frac{4\pi\alpha^2 d\alpha}{\delta_x \delta_y \delta_z}$
Charge density in real space	$\rho(x) = \frac{en_o}{2\delta_x} \int^\infty \delta(\alpha^2 - F_o + \frac{x^2}{\delta_x^2}) \frac{d\alpha^2}{\alpha}$ $= \frac{en_o}{2\delta_x} \frac{1}{\sqrt{F_o - \frac{x^2}{\delta_x^2}}}$	$\rho(x,z) = \frac{\pi e n_o}{\delta_x \delta_z} \int^\infty \delta(\alpha^2 - F_o + \frac{x^2}{\delta_x^2} + \frac{z^2}{\delta_z^2})\, d\alpha^2$ $= \frac{\pi e n_o}{\delta_x \delta_z}$	$\rho(x,y,z) = \frac{2\pi n_o}{\delta_x \delta_y \delta_z} \int_o^\infty \delta(\alpha^2 - F_o + \frac{x^2}{\delta_x^2} + \frac{y^2}{\delta_y^2} + \frac{z^2}{\delta_z^2})\, \alpha d\alpha^2$ $= \frac{2\pi n_o}{\delta_x \delta_y \delta_z} \sqrt{F_o - \frac{x^2}{\delta_x^2} - \frac{y^2}{\delta_y^2} - \frac{z^2}{\delta_z^2}}$
Integral formula	$\int_o^\infty \frac{\delta(x - a)}{\sqrt{x}}\, dx = \frac{1}{\sqrt{a}}$	$\int_o^\infty \delta(x - a)\, dx = 1$	$\int_o^\infty \delta(x - a)\sqrt{x}\, dx = \sqrt{a}$
Uniform?	no!	yes!	no!

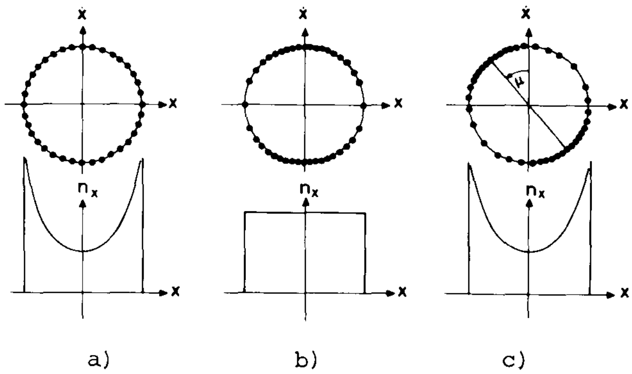

Fig. 3 a) Uniform surface charge density on phase space ellipse. Inhomogeneous charge distribution in real space

$$n_x \sim \frac{1}{\sqrt{1 - x^2}}$$

b) Inhomogeneous surface charge density on phase space ellipse. Uniform charge distribution in real space.
c) Rotated phase space ellipse after transfer over optical period, angle μ. Phase space and real space distributions both inhomogeneous.

Thus the 6-dimensional hyperellipsoid of Table 1 is not capable of producing a 3-dimensional uniform charge distribution. Both models prove non-physical. In one case, one trades conservation of uniformity for the sacrifice of a dimension, while in the other, uniformity must be abandoned because of the requirement for 3-dimensions.

Computational Results

The computations presented in this paper took into account mainly model 2, in spite of the lack of self-consistency mentioned, because of the considerable deviations associated with the extraordinary factor 2 in (2a) due to the plane wave assumption. Effects of different form factors, (3a) and (3b) cause less severe deviations. Fig. 4 shows a maximum decline at $a_x = a_z$ with 0.5 (3a) compared to 0.33 (3b), whereas both form factors merge at $a_x << a_z$ and $a_x >> a_z$.

As a linac (neglecting any practical realization at the moment) a chain of rf-resonators (helix, spiral, splitring, etc.) is favored. The scheme is shown in Fig. 5. Focusing should be provided by superconducting coils wound on the resonator tanks.

Data are summarized in Table 2.

For the calculations, a computer program has been developed, which gives the axial and radial synchrotron acceptances of the first section, using equations (1), (2b), (3b). Envelope radii required for the solutions of (1), (2b) are computed iteratively, where the chargeless case Q = 0 is taken as a zero approximation. Elements

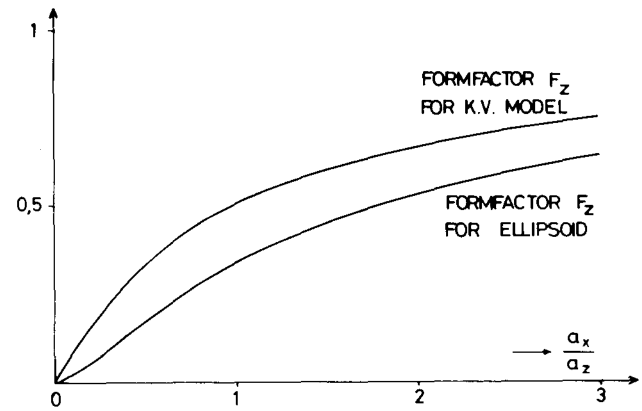

Fig. 4 Form factors for K-V model and ellipsoid

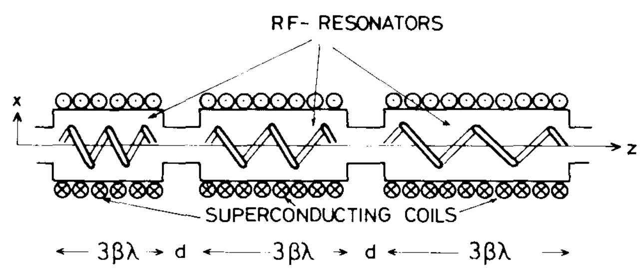

Fig. 5 Scheme of the linac considered

Table 2

Particle:	$^{2}_{130}$Xe
Initial energy:	1 MeV
Final energy:	23.4 MeV
Constant voltage gain per section:	0.28 MV
Linac frequency:	13.5 MHz
Number of sections:	40
Synchronous phase:	30° (45°)
Initial axial envelope:	30°
Section length:	3βλ
Drift length:	10 cm

of all beam transports form WKB transfer matrices[10]. A more detailed report on this computer program will soon be published. It should additionally be noted that the basic implied postulate of identical emittance areas[1] with respect to both motion components is not included in this paper. For that, a further iteration procedure is required, for which work has started.

The program obviously admits similar computations of Wideroe (βλ/2) and Alvarez (βλ) structures.

Figure 6 shows a typical slope of acceptances with bunch charge, where Q = 10^{-10} C corresponds to a particle current of 4.22 • 10^{15} particles per second (duty factor 1).

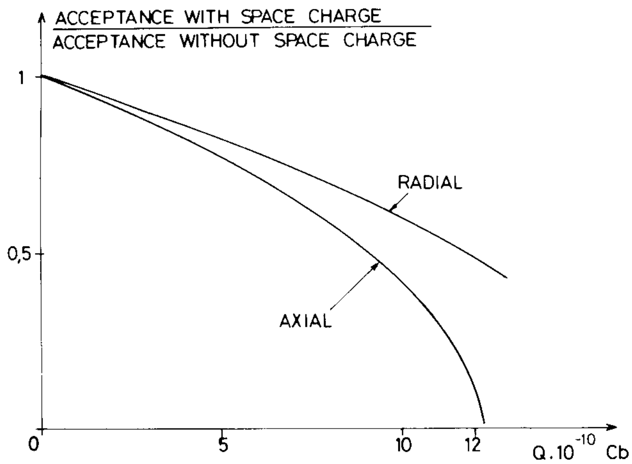

Fig. 6 Decrease of acceptances with space charge. 10^{-10} C $\hat{=}$ 4.22 • 10^{15} particles/s. Radial envelope radius 1 cm.

Defining "maximum" charge as the one which reduces the smaller of the two acceptances to 50% with respect to the chargeless case, Fig. 7 indicates an extraordinary behavior, caused by the aperture dependence in the form factor (3b) of Fig. 4. Here this maximum charge is shown versus the radial aperture indicating that restriction of maximum charge is due to axial losses at large apertures, independent of the focusing field. Improvement with a stronger magnetic field is only seen at smaller apertures. This coupling effect of both motions, where coupling is exclusively caused by space charge effects, is more obvious in the next figure. As Fig. 8 indicates, charge and magnetic pressure, when sufficiently high, give rise to a squeezing effect to such an extent that the beam moves axially, where the pressure is less. Thus a tendency to incompressible behavior is observed, causing instabilities especially due to envelope coupling effects, as the magnetic field does not show up explicitly in the axial equation (1). With regard to the case with zero space-charge, Flocquet exponents range from μ_o = 30° at 11 Tesla up to μ_o = 80° at 22 Tesla.

Figure 9 shows an example of beam envelope in a long linac, data being given in Table 2. Here axial and radial beam envelopes are traced through 40 sections. Due to a rather moderate acceleration field, the phase oscillation amplitudes are increasing in the first sections, damping being delayed due to space-charge. Several pairs of envelopes which were considered, give an explanation of the beam behavior, namely; a strong envelope coupling between axial and radial motions after starting together with a rather unfavorable development of the axial Flocquet exponent. Axial and radial amplitudes turn out similar. The electrical field together with a more advantageous synchronous phase is increased, but still damping of phase oscillations is essentially prevented by

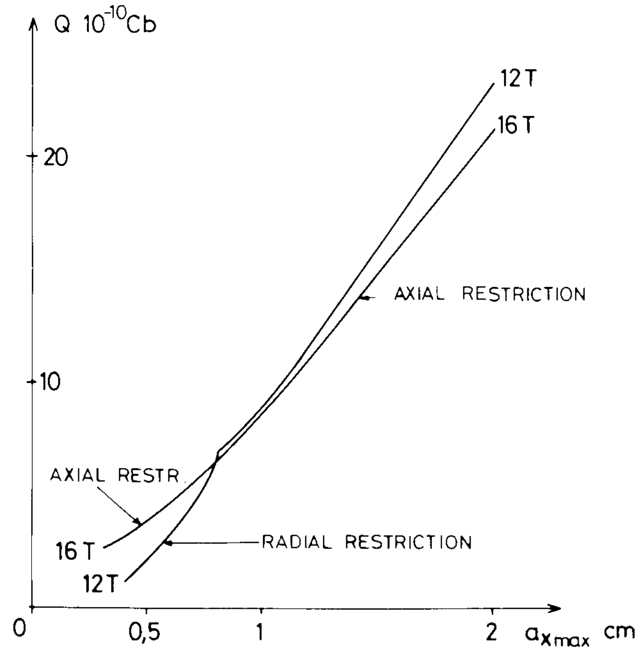

Fig. 7 Typical aperture dependence of maximum charges at two magnetic focusing fields.

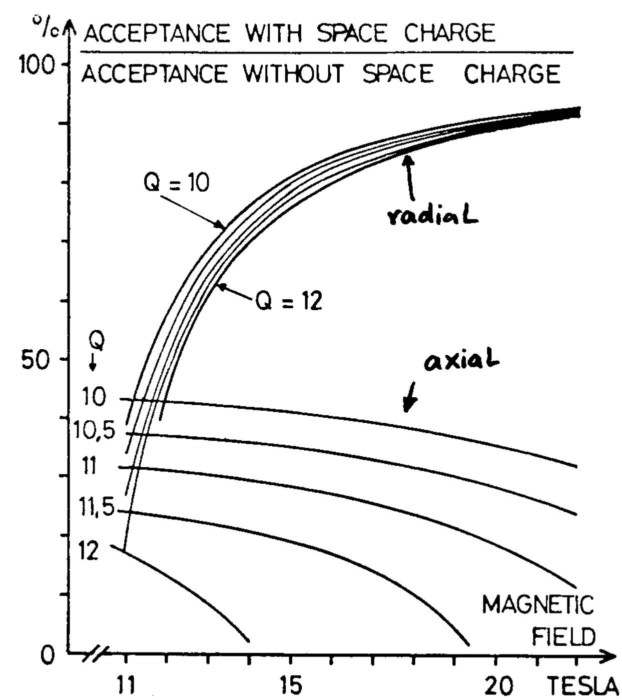

Fig. 8 Squeezing effect of strong magnetic field on axial acceptance. Radial envelope radius 1 cm.

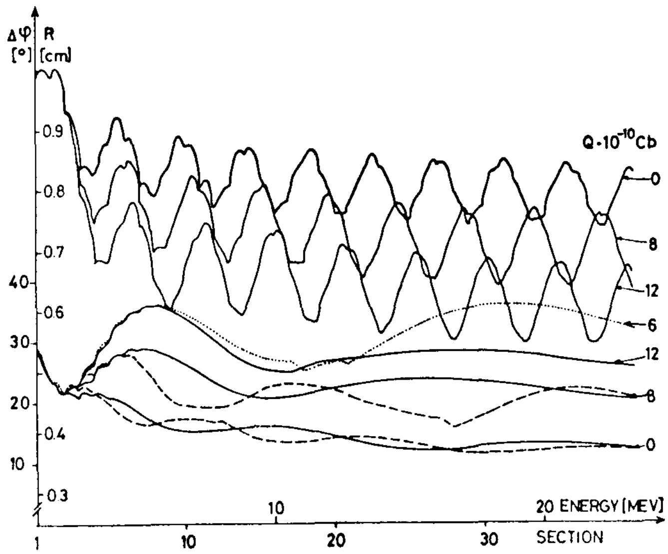

Fig. 9 Radial (above) and axial (below) envelope behavior at several bunch charges

space-charge, as the dashed curves indicate. For a comparison of the two models, the dotted curve illustrates even a more unfavorable beam behavior in case of Model 1. Doubling of rf at high space-charge should be handled with utmost care, since extrapolation of zero space-charge situations seems dangerous.

Conclusion

In the future, an iteration routine for identical emittances will be included, as dictated by the K-V formalism. The extension to 3-dimensions will be pushed forward, and a fast subroutine for numerical calculation of elliptic integrals will be installed. Investigations shall be extended to periodic linacs like Wideroe and Alvarez. Finally the model will be tested using data of existing proton linacs as well as other multiparticle programs. This might support an rms formalism for axial motion with regard to the model discussed in this paper.

Acknowledgements

We want to thank Mr. K.-D. Halfmann for his valuable help in computer programming. Work was supported by the Bundesministerium fur Forschung und Technologie. Computations have been carried out at HRZ at the University of Frankfurt/Main.

References

1 J.M. Kapchinskij, V.V. Vladimirskij, Limitations of proton beam current in a strong focusing linear accelerator associated with the beam space charge, Proc. Intern. Conf. on High Energy Acc., CERN, Geneva, p. 274 (1959).

2 M. Reiser, Periodic focusing of intense beams, Part. Acc., Vol. 8, p. 167 (1978).

3 F.J. Sacherer, rms envelope equations with space-charge, CERN/SI/Int. DL/70-12, 1970.

4 P.M. Lapostolle, Quelques proprietes essentielles des effets de la charge d'espace dans les faisceaux continus, CERN-ISR/DI-70-36, 1970.

5 G. Wendt, Statische Felder und stationäre Ströme, in: S. Flügge, Handbuch der Physik, Springer, Berlin-Göttingen-Heidelberg 1958, p. 148.

6 K. Mittag, On parameter optimization for a linear accelerator, KFK 2555, Karlsruhe, January 1978.

7 R.W. Muller, Space-charge current limits in linacs, Internal paper, GSI Darmstadt, autumn 1978.

8 E.D. Courant, H.S. Snyder, Ann. Phys., 3 (1958) p. 1.

9 P. Junior, Ein Theorem zur radialen Fokussierung von Strahlfuhrungssytemen mit wenigen Wiederholungen, Z. f. angew. Phys., 28 (1970) pp. 353 - 357.

10 P. Junior, Die Optimierung der Fokussierung unperiodischer Linearbeschleuniger, Hab.-Schrift, Inst. f. Angew. Physik, Universitat Frankfurt/M., 1969, unpublished.